T.3: Microstructure-texture-magnetization correlation in spinel ferrite thin films

Lakshmikanta Aditya,
Ferrite Technology Laboratory, Acclerator Magnet Technology Division,
(aditya@rrcat.gov.in)

1. Introduction

The integration of magnetic thin films with other semiconductor process technology has led to a heightened interest in thin film ferrite processes. Recent developments in thin film growth and characterization techniques have stimulated further research interest on ferrite thin films because of their potential applications in miniaturized high-frequency devices, magneto-optical memory devices, sensors, microwave monolithic integrated circuits and spintronics. Such applications of these functional magnetic materials are driven by their macroscopic physical properties like magnetization, coercivity and permeability. Magnetization is an intrinsic property while the other two are microstructure dependent extrinsic properties. Magnetic superexchange interaction between the cations in tetrahedral (A) and octahedral (B) sublattices through the intervening oxygen anions in spinel structure (AB_2O_4) leads to ferrimagnetism, and the resulting vector sum of magnetic moments on the two sublattices defines the value of magnetization of a spinel ferrite. The cation occupancy on the various crystallographic sublattices are decided by various factors including ionic radii, size of the sublattices, orbital preference of specific co-ordination, process temperature and the subsequent cooling rate and are well established in bulk ferrites [1]. However, in most ferrite thin films magnetization is observed to be lower than the corresponding bulk values - an aspect which has not been understood well.

In conventional single-phase polycrystalline materials, any microstructure dependent property is determined by size, shape and orientation of the grains. The type- and frequency of grain boundaries, so called 'grain boundary character distribution (GBCD)', though crucial in inter-granular properties, may not affect bulk properties significantly [2]. Role of grain boundaries is expected to gain significance in materials with 'reduced' grain sizes, such as nano-crystalline materials and thin films. Although magnetization is an intrinsic parameter, deviations in nanocrystalline ferrites may arise owing to grain size [3], GBCD [2] and cation distribution in the sublattices[1].

Generally, thin films have higher defect densities than the corresponding bulk materials. The defects that are generally seen in polycrystalline thin films are grain boundaries, column boundaries, voids, vacancies, dislocations and gas-bubble inclusions. As the grain boundaries occupy a significant volume in thin films, it is reasonable to anticipate that for the same grain size, chemical phase and composition, properties might change remarkably when the grain boundary structure is altered. During the deposition or post-deposition thermal treatments of the nanocrystalline films, grains grow along with manifestation of some sort of textures. These crystallographic textures are related to specific grain boundary structures or GBCD. Since most practical miniaturized magnetic devices will be built on polycrystalline materials with nanometric grain sizes, such as polycrystalline ferrite thin films, a systematic study of ferrite thin film processing and resulting microstructures is obviously interesting from the viewpoint of their macroscopic physical and magnetic properties.

2. RF sputtered Li-Zn ferrite films:Magnetization in relation to grain boundary natures

Microstructural origin of lower magnetization have been investigated in Li-Zn ferrite thin films. Microstructural changes have been brought about by varying Zn concentrations.Li-Zn ferrite ($Li_{0.5-x/2}Zn_xMn_{0.1}Fe_{2.35-x/2}O_4$, with x = 0.0, 0.16, 0.32, and 0.48) thin films of thickness between 300 to 400 nmwere deposited on Si(100) substrates at ambient temperature by RF sputtering of corresponding ceramic targets using a Leybold Z400 system. These films were subsequently annealed at 850°C in air atmosphere with very slow cooling rate to ensure inverse spinel phase formation by thermodynamic stabilization of cation distribution between crystallographic sub-lattices [4].

These films were characterized thoroughly by VSM (vibrating sample magnetometer), XRD (X-ray diffraction), TEM (transmission electron microscopy) and AFM (atomic force microscopy). The crystallographic texture studies of the films were performed by measuring four X-ray pole figures and orientation distribution function (ODF) and inverse pole figures were computed using standard series expansion techniques [5].

In-plane M-H data of Li-Zn ferrite thin films(Fig. T.3.1) shows that film magnetization do not saturates even at an applied field of 8 k-Oe. Hence the spontaneous magnetization ($4M_{ST}$) of the films have been computed using linear intercept method. $4M_{ST}$ and coercivity (H_C) data of the films are presented in Table T.3.1 along with corresponding bulk values. The coercivity of the films are observed to be higher than the corresponding bulk values by an order of magnitude, whereas magnetization values are considerably lower. The percentage reduction of the film magnetization from corresponding bulk ($_M$) has been calculatedand shown also in TableT.3.1. $_M$ variation with x is not monotonous. $_M$ is observed to decrease sharply with increasing Zn concentration (x)

with a minima (17.78%) at x = 0.32. Further increase of x till 0.48 leads to sharp increase of δ_M.

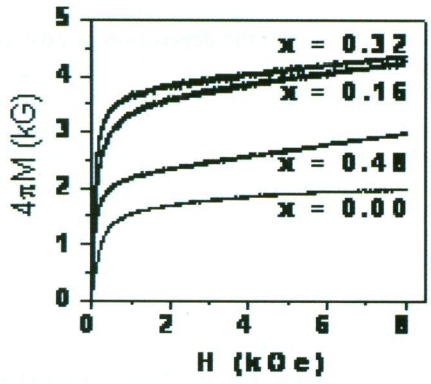

Fig.T.3.1. In-plane, room temperature recordedinitial magnetization curves of Li-Zn ferrite thin films for different Zn concentration (x)

Table T.3.1. Magnetic properties of Li-Zn ferrite thin films in compare to corresponding bulk

Zn Conc	Bulk		Film		4πM deviation
(x)	$4\pi M_S$ (G)	H_C (Oe)	$4\pi M_{ST}$ (G)	H_C (Oe)	δ_M (%)
0.00	3600	2.3	1868	142	48.1
0.16	4600	1.6	3750	62	18.5
0.32	4800	0.8	3950	39	17.7
0.48	4000	0.6	2167	23	45.8

Energy-dispersive X-ray analysis (EDX) and electron probe microanalysis (EPMA) studies have shown that these Li-Zn ferrite films have similar compositions to those of the corresponding targets. Structural studies using selected area electron diffraction (SAED) and XRD show development of well-crystallized spinel LiZn ferrite structure. Monotonous decrease of grain size with increasing x, as observed from TEM and AFM measurements,may not explain the observed variation of $_M$. Slow thermal annealing at 850°C ensured inverse spinel phase stabilization in the films as in bulk which suggests that the cation distribution in the films are similar to corresponding bulks. The values and the trend of Curie temperature (T_C) in these films are shown to be similar to those of the corresponding bulks. Hence, various exchange constants might have similar values in bulks and in the corresponding films. Hence these are not responsible for $_M$ variation with x. Fitting of high-field magnetization data to the Chikazumi model [6] yields anomalous variation of high field susceptibility (H^*) with x. The trend of H^* and $_M$ with x is neither similar not reverse. This makes us to believe that $_M$ is not influenced by high field susceptibility in these films.

Macrotextureanalysis using X-ray ODF and IPFs, however, show a reverse trend in the extent of crystallographic texturing, as shown in Fig. T.3.2.The texture indexclearly increased till x=0.32 and then dropped significantly as x further increases to 0.48.

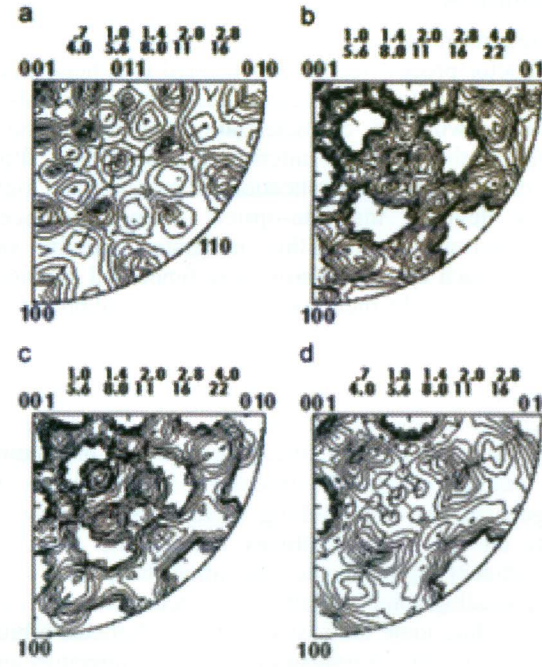

Fig.T.3.2:IPFs representing textures of the Li-Zn ferrite thin films with varying Zn conc.: a) x = 0.00, b) x = 0.16, c)x = 0.32 and d) x =0.48.

Uncorrelated low angle grain boundaries (LAGB), as computed from the discretized X-ray ODF data, show similar trend of texturing but reverse trend of $_M$ with varying Zn concentration. Correlated LAGB's were computed from the micro-texture measurements using TEM based orientation imaging microscopy (OIM) and are found to be in good agreement with those obtained from X-ray ODF data, as shown in Fig. T.3.3. At x = 0.32, $_M$ is the least with a maxima in LAGB and at x = 0.00, $_M$ is the largest with a minima in LAGB. Increase in low angle, and hence low energy, grain boundaries decreases $_M$ as x increases from 0 to 0.32. As x increases beyond 0.32, the low angle boundary concentration drops significantly resulting in sharp increase of $_M$. For the first time, the deviation of film magnetization from its bulk value ($_M$) is correlated to grain boundary character distribution in the sputtered Li-Zn ferrite thin films [7].

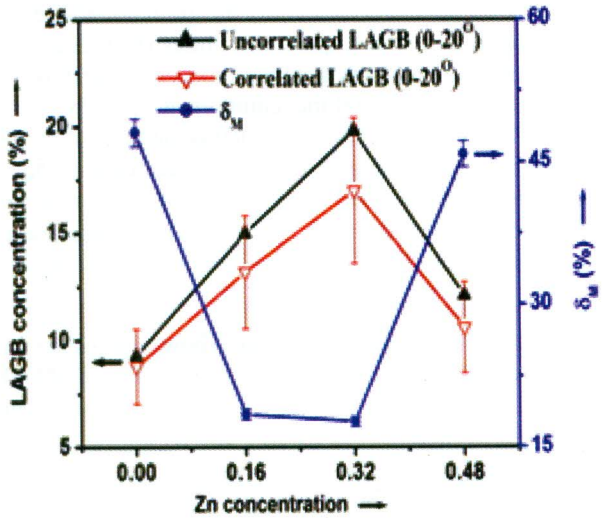

Fig.T.3.3: $_M$ and low angle grain boundaries as a function of Zn concentration.

1. Laser ablated cobalt ferrite thin films: Microstructure-magnetization correlations

The microstructural changes in the multi-component Li-Zn ferrite thin films were introduced by varying Zn concentration, and the correlation between $_M$ and GBCD was based on the statistics of four samples. In order to examine microstructure dependence of $_M$ in inverse spinel ferrite films, a binary $CoFe_2O_4$ was studied extensively with extended correlation statistics. The microstructural changes were brought about in these films by varying substrate deposition temperature (T_S), film thickness, annealing temperature (T_A) and annealing time. Slow thermal annealing process was maintained in all the grain growth experiments to ensure inverse spinel phase stabilizationin cobalt ferrite films.

3.1 Influence of substrate temperature and post deposition thermal treatment

Pulsed laser deposited (PLD) cobalt ferrite ($CoFe_2O_4$) thin films of thickness 140 (10) nm were grown on amorphous fused quartz substratesat different T_S (25 -750°C). A 3rd harmonic (355 nm) Nd:YAG laser with 10 Hz repetition rate, 5 – 6 ns pulse width and 2.5 J/cm^2 laser fluence was used to ablate a rotating $CoFe_2O_4$ceramictarget in oxygen pressure of 0.16 mbar. Structural studies of the films were performed using XRD, AFM, TEM and micro-Raman spectroscopy. Crystallographic bulk texture measurements of the films were performed by measuring (111), (311) and (511) pole-figures in the polar angle ranging from 0 to 85 and the azimuthal angle ranging from 0 to 360using a standard four-circle automatic texture goniometer equipped withPANalytical'sX'Pert PRO MRD X-ray diffractometer. Orientation distribution function and inverse pole figures (IPF) have been computed from the measured X-ray pole figures taking cubic crystal symmetry and orthorhombic sample symmetry into account and using the Arbitrarily Defined Cells method [8].

Cobalt ferrite thin films grown at room temperature show no XRD peaks. However, SAED studies show polycrystalline spinel phase formation in the film. Micro-Raman investigation shows octahedral and tetrahedral Raman modes which indicate formation of octahedral and tetrahedral sublattices in the room temperature grown film. Observed inverse grain size dependency of Raman line broadening and Raman line asymmetrystrongly suggest increasing lattice disorder with decreasing grain size. This implies presence of very high defect density in the room temperature grown cobalt ferrite thin film. As the film was grown at ambient temperature, the quenching rate of the ablated plume was so high on substrate surface that the thermal energy available for crystallization was insufficient leading to formation of distorted spinel. Conventional -2XRD measurements reveal (111) preferred orientation in the as-deposited films with a T_S 300C. Crystallographic texture measurements using X-ray ODF confirmed (111) texturing with increasing texture intensity as T_S increases from 300C to 750C, as shown in Figs. T.3.4a.AFM studies showsrelatively better surface quality in 750°C deposited film. Grain size estimation using grazing incidence X-ray line broadening analysis shows insignificant grain growth with increasing T_S, which is in good agreement with grain size data obtained from bright field TEM imaging [9].

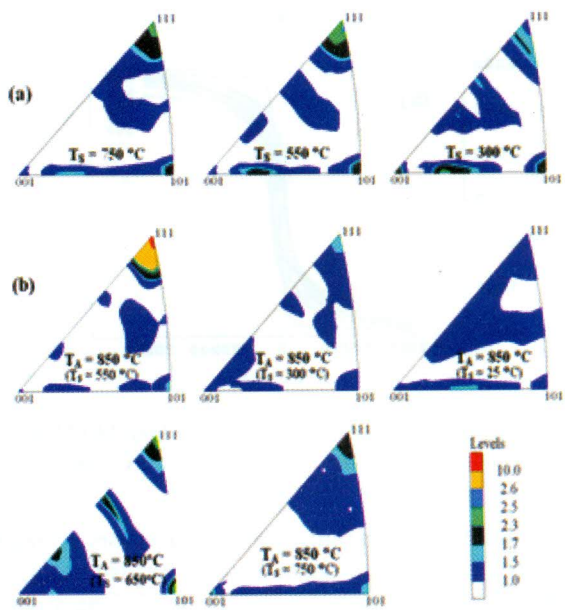

Fig.T.3.4:001 IPFs showing textures of the (a) as-grown and (b) 850°C-annealed $CoFe_2O_4$ thin films.

After annealing in air at 850C, the (111) textures were retained, but the trend of texturing with T_s is observed to change significantly, as shown in Fig. T.3.4(b). Conventional θ-2XRD measurements of the annealed films as well as bulk texture measurements using X-ray ODF reveal strong (111) preferred orientation in the film grown with a T_s of 550°C (Fig. T.3.4b).

In-plane magnetic measurements were carried out at 300 K using a VSM of Quantum design PPMS system. The M-H loopsof the as-grown and the annealed filmsin compare to the bulk targetare shown in Fig. T.3.5.As seen, the film magnetization does not saturate even an applied field of 5 Tesla. Spontaneous magnetization of the films have been computed and the corresponding$_M$ values have been calculated. Monotonic increase of $4\pi M_{ST}$with increasing $T_s$is observed in as-grown films.However, the annealed film with aT_s of 550C shows a maxima in $4M_{ST}$ which is close to the bulk saturation magnetization.

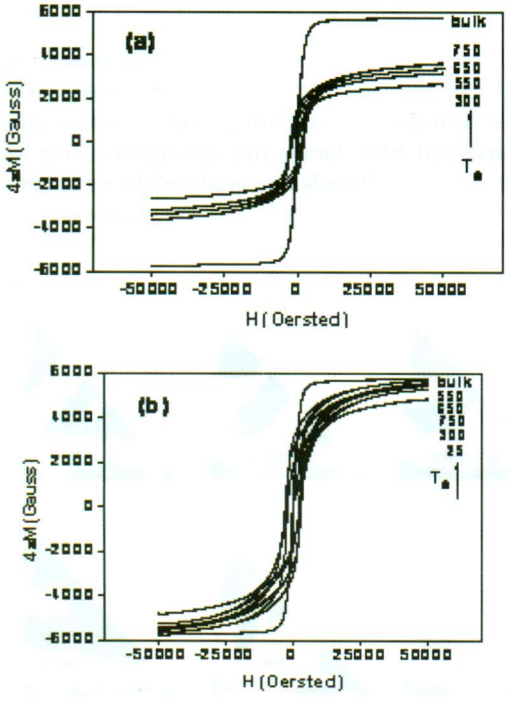

Fig. T.3.5: Room temperature recorded in-plane M-H loops of the (a) as-grown and (b) the annealed films, as compared to bulk

The δ_M valuesof as-grown films are observed to vary inversely with grain size and maximum texture intensity, $f(g)_{MAX}$. Computation of inter-crystalline components using a phase mixture model shows significant decrease of inter-crystalline components (43 % to 18 %) as a result of grain growth from ~ 6 nm (for T_s = 25°C) to 16 nm (for T_s = 750°C). These inter-crystalline components are mainly the grain boundaries (f_{GB}), triple junctions (f_{TJ}) and quadratic nodes (f_{QN}), and are the regions of major defects in the nanocrystallinefilms. With reduction of inter-crystalline components and hence with increase of crystallites, the spontaneous magnetization of the films increases resulting in monotonic decrease of δ_M with increasing T_s. Monotonic increase of $f(g)_{MAX}$i.e., monotonic increase of texture index with T_s results in monotonic increase of LAGB's resulting in further decrease of δ_M with increasing T_s.

TEM studies ofthe annealed films show significant grain growthwith grain size maxima achieved at a T_s of 550°C (Fig. T.3.6). The film with a T_s of 550°C shows maxima of grain size 66 nm, residual stress 13 GPa and $f(g)_{MAX}$10. The sharp maxima of $f(g)_{MAX}$ for the T_s550°C film indicates significant reduction of defect concentration in this film which is clear from the dislocation density estimation using high resolution X-ray line profile analysis. Observed reduction of grain size and residual stress in the film for T_s> 550°C is thought to arise from the reduction of effective annealing temperature, ΔT (= T_A-T_s), the driving force for grain growth. For such grain growth, both defect density and grain boundary energy can act as the driving force. The mechanism of high angle boundary movement being a thermally activated process is, however, expected to depend on ΔT. An alternate explanation for the observed stress relaxation and lower grain size, may come from plastic deformation during annealing and corresponding grain refinement.

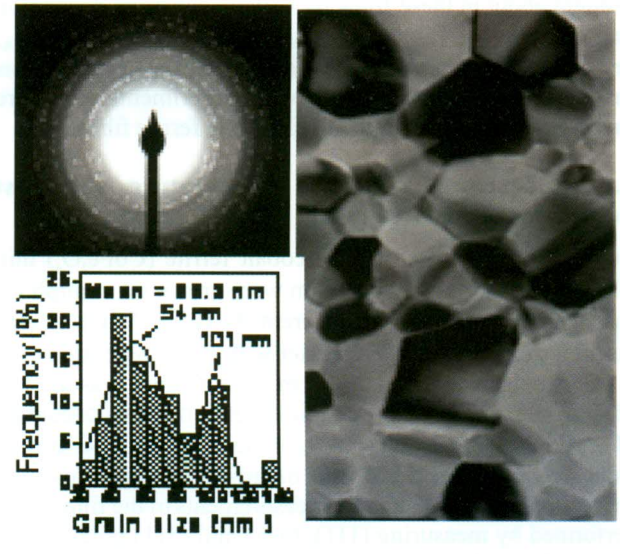

Fig.T.3.6: Bright field TEM image of the 850°C annealed film grown with a T_s of 550°C.SAED pattern and grain size distribution are shown in the inset.

T_S dependence of $_M$, grain size and $f(g)_{MAX}$ of 850°C-annealed films are shown in Fig. T.3.7. δ_M now follows a reverse trend with grain size and $f(g)_{MAX}$ as a function T_S. Grain size variation in the film for T_S> 300C is not very significant. Variation of $f(g)_{MAX}$ is very significant at a T_S of 550°C. The minima of δ_M at a T_S of 550°C is observed to be associated with a maxima of $f(g)_{MAX}$. Since, all the films were thermally annealed at the same annealing conditions, the cation distribution may not change significantly and thus it will not influence the observed magnetization values. Since grain size variation for T_S> 300°C is not very significant, the trend of δ_M with T_S cannot be explained in the light of grain size alone. Inverse $f(g)_{MAX}$ dependence of δ_M suggests that δ_M and LAGB follow reverse trend in 850C-annealed cobalt ferrite films. Hence, $_M$ variation with T_S might be ascribed to LAGB. $_M$ is correlated to GBCD in the 850C-annealed cobalt ferrite thin films.

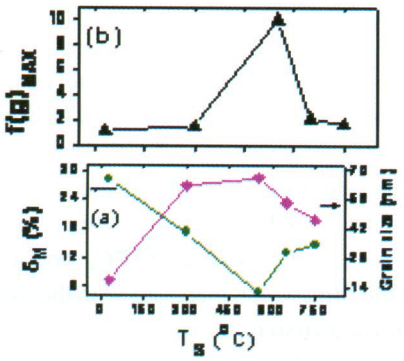

Fig. T.3.7: T_S dependence of microstructural and magnetic parameters in 850C-annealed films: (a) $_M$ and grain size, and (b) $f(g)_{MAX}$.

3.2 Thickness effecton Texture and Magnetization

Further, we have focused on the effects of film thickness on structural, textural, microstructural and magnetic properties of the as-grown and the annealed cobalt ferrite films to establish a correlation between$_M$ and the structural properties. Since the substrate deposition temperature was optimized and found to be 550C, therefore, in this work laser ablated cobalt ferrite thin films of various thicknesses (40- 300 nm) were grown at 550C on amorphous fused quartz substrates. A set of the as-grown films were annealed at 900C. Monotonic increase of texture intensities with increasing film thickness of the as-deposited and annealed films, as shown in Fig. T.3.8, can be attributed to selective growth process dominated by reduced defect density. As-deposited films shows decreasing Raman line asymmetry with increasing film thickness thereby confirming reduced lattice disorder as film thickness increases [10].SAED patterns of the films (Fig. T.3.9) shows polycrystalline spinel structure, although this was not very clear from XRD patterns of the thinner as-deposited films. Grain growth is observed to be very significant upon annealing as seen from the bright field TEM images.

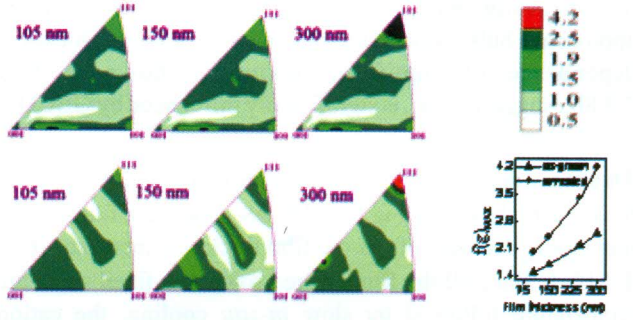

Fig.T.3.8:001 IPFs showing thickness dependence of texture of the a) as-deposited and b) annealed films. Figure c shows $f(g)_{MAX}$ as a function of film thickness.

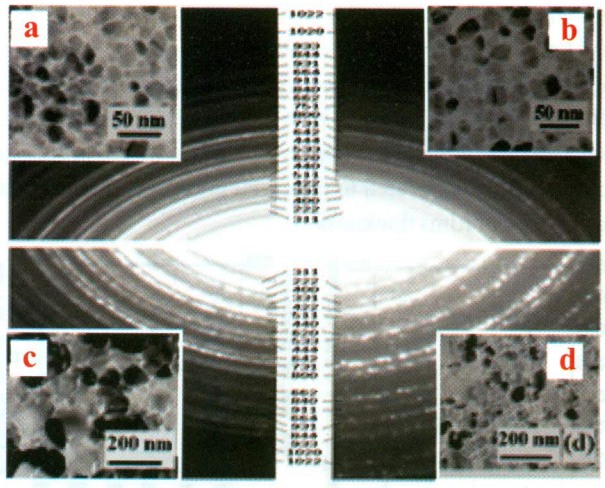

Fig.T.3.9: SAED patterns of the as deposited cobalt ferrite films of thickness (a) 300 nm and (b) 60 nm & annealed films of thickness (c) 300 nm and (d) 60 nm.Bright field images are shown in the inset.

Magnetic properties have been determined from the in-plane M-H measurements. Thickness dependent H_C data are consistent with the behavior of nano-crystalline systems wherein H_C is observed to increase with increasing grain-size in the single domain regime. For as-deposited films, H_C reduction beyond the film thickness of 150 may be attributed o reduction of interface stress. The coercivity of the annealed films is observed to increase with increasing grain-size till a

t critical grain-size beyond which the particles become multi-domain. The domain-wall movements in multi-domain particles results in a reduced coercivity with further increasing grain-size.Magnetization of the900°C-annealed cobalt ferrite films are also observed to increase monotonically with increasing film thickness, and it approaches bulk value at the thickness of 300 nm.Thickness dependence of significant texturing shown in Fig. T.3.8b,csuggests that $_M$ is significantly influenced by GBCD.

Thickness dependence of $_M$ and microstructural parameters have been shown in Fig. T.3.10. As-deposited films show monotonic decrease of $_M$as the film thickness increases (Fig. T.3.10a]. Since all the films were grown at a fixed substrate temperature followed by slow *in-situ* cooling, the cation distribution is also not expected here to change with film thickness. Hence, $_M$ variation with film thickness might be ascribed to grain growth, reduced defect density and increasing texturingof the as-deposited cobalt ferrite thin films.The similar trend of $_M$ is observed in case of annealed films also, as shown in Fig. T.3.10b.The observed reverse trend between $_M$ and grain size with increasing film thickness, suggests that the magnetization of our annealed films are also grain size dependent. Hence, with increasing film thickness, $_M$ decreases monotonically whereas texture index and grain size increases. δ_M is correlated to observed grain size & LAGB in as a function of films thickness.

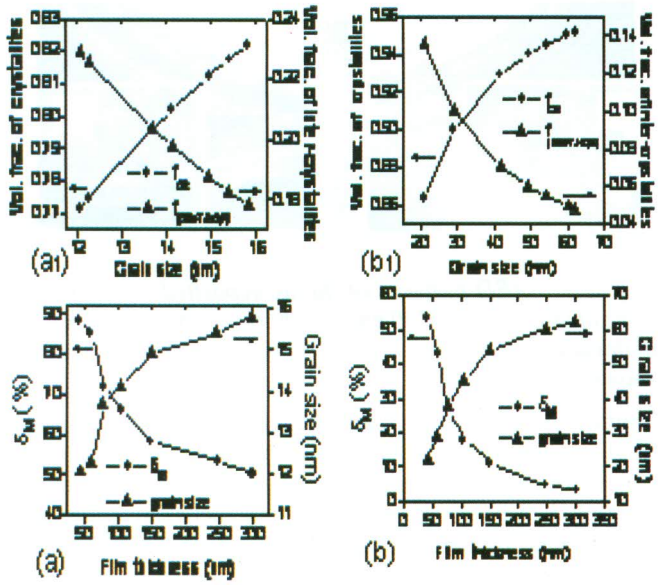

Fig.T.3.10:$\delta_M$and grain-size as a function offilm thickness for (a) as-deposited and (b) annealed films. Thickness dependent vol. fraction of crystallites & inter-crystallite components for the two cases are shown in Figs (a_1) and (b_1) respectively.

4. RF Magnetron sputtered cobalt ferrite films

Finally, we have focused on the structure-property correlations in the rf magnetron sputtered cobalt ferrite thin films (250 10 nm) on amorphous fused quartz substrates. These films were grown at ambient temperature with a high rf power of 240 W, and subsequently thermally annealed at different temperature (550 – 1150°C). These films were also annealed at 1050°C for different time (15 minutes to 32 hours).The process parameters like high rf power (240 W), large target to substrate distance (9 cm) and slow thermal annealing results in the synthesis of non-textured polycrystalline films which enable us to compare microstructure dependence of $_M$ with textured cobalt ferrite thin films.

Significant changes in residual stress are observed upon increasing the annealing temperature (T_A). The films annealed at 650°C show tensile stress of 6.5 GPa. As T_A increases to 750°C, compressive stress (-7.5 GPa) is generated in the film which relaxes to -2 GPa as T_A increases to 850°C. Upon further increase of T_A beyond 850°C, tensile stress is developed in the film, which increases with the increase of T_A till 1050°C. Beyond 1050°C, the residual stress relaxes as T_A is further increased. With increasing soaking time (keeping T_A fixed at 1050°C), monotonic relaxation of residual tensile stress is observed. XRD and micro-Raman studies show significant structural changes upon thermal annealing. The average cation-oxygen bond length, as estimated from micro-Raman data, has been correlated to the out of plane lattice parameter as well as the residual stress.

In-plane M-H loops of cobalt ferrite films annealed at different temperatures, are shown in Fig. T.3.11a. The observed spontaneous magnetizations in our films are 43 % to 85% of bulk value depending on the annealing temperatures. The observed trend of coercivity as a function of grain size, as shown in Fig. T.3.11b,c, may be explained on the basis of grain-size dependency of coercivity in the single domain and multi-domain regime.

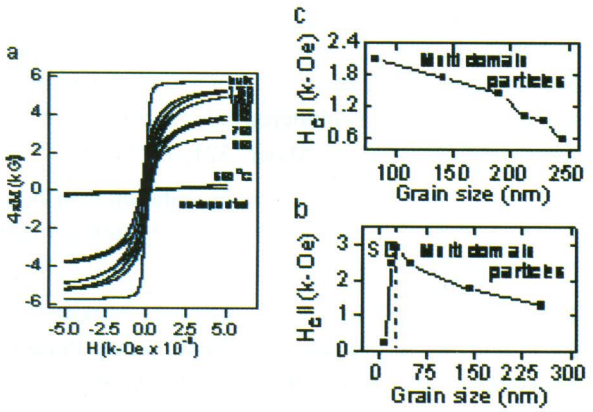

Fig.T.3.11:a) In-plane M-H loops of the films annealed at different temperatures.Grain-size dependence ofcoercivity of the films (b) annealed at different temperatures and (c) annealed for different times

The nature of the room temperature isotherms of $(4M)^2$ vs. H/Mor the Arrott plots of the as-deposited and 550°C-annealed films are indicative of higher defect concentration of the films. A low field tail in the Arrott plots is observed to narrow with increasing annealing temperature and time and almost vanishes after an annealing duration of 32 hours. This indicates that increased structural homogeneity is achieved with increasing annealing temperature and time. In other words, decreasing defect density with increasing annealing temperature or time is observed. This, in turn, favors increased film magnetization.

Grainsize dependence of δ_M values have been shown in Fig. T.3.12. Grain size and δ_M values are observed to change monotonically with increasing annealing temperature but follow opposite trend to each other, as is shown in Fig. T.3.12a. The influence of annealing duration on δ_M is very significant for initial 2 hours, (Fig. T.3.12b.) In both cases, the volume fraction of the intercrystalline components ($_{GB+TJ+QN}$) are observed to be reduced significantly with increasing annealing temperature and time, as shown respectively in Figs. T.3.12-a_1 and -b_1. The reduced concentration of these defects are expected to increase film magnetization resulting corresponding decrease of $_M$ values.

No texturing with annealing temperature or annealing time has ruled out any correlation between δ_M and GBCD. Although cation distribution in spinel sub-lattices may be altered with varying annealing temperature, this can be controlled by slow cooling after post-deposition annealing. Cation distribution in the tetrahedral and octahedral sub-lattices in the films are similar to those of the corresponding bulks because of inverse spinel structure and hence will not affect the δ_M values. Hence, in our rf magnetron sputtered cobalt ferrite thin films, δ_M reduction with increasing annealing temperature or annealing time may be ascribed mainly to increasing grain size and reduced defect concentration.

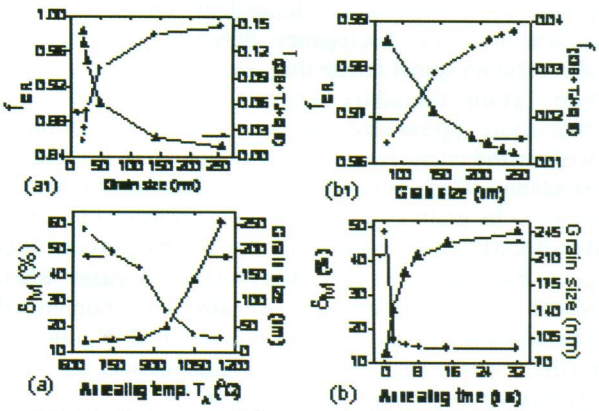

Fig.T.3.12: Variation of δ_M and grain size as a function of (a) annealing temperature and (b)annealing time. Grain size dependent volume fraction of crystallites and inter-crystalline components for the two cases are given in figure (a_1) and (b_1) respectively.

5. Microstructure-texture-$\delta_M$correlation

A comparison of $_M$ values of the non-textured films to those of (111) textured laser ablated films with similar grain sizes shows significantly higher $_M$ values in non-textured cobalt ferrite films. Further a comparison of textured and non-textured films with similar grain size shows that $_{M\text{-SPUTTERING}}$ (non-textured) $>_{M\text{-PLD}}$(non-textured) $>_{M\text{-PLD}}$(textured), as shown in Table T.3.2.Since $_M$ values of the non-textured sputtered films were considerably larger, these films were annealed at further higher temperatures till 1150C to see if $_M$ decreases merely by increasing grain-size. However, the $_{M\text{-SPUTTERING}}$ does not reduce below 15% even after annealing at1150C that corresponds to an average grain-size of 245 nm. For 250 nm thick films, $_{M\text{-SPUTTERING}}$[non-textured] is observed to be higher by 10% as compared to $_{M\text{-PLD}}$[(111)textured] in spite of significantly larger grain-size of the former. This study clearly establishes the role of textures in influencing the magnetization of nano-crystalline cobalt ferrite thin films.

Table T.3.2: $_M$ data of $CoFe_2O_4$ films

Parameters	Non - textured RFMS film	Non - textured PLD film	(111) Textured PLD film	(111) Textured PLD films
T_A (°C)	950	850	900	850
Thickness(nm)	250	140	150	140
Grain-size(nm)	49	62	54	66 54 46
δ_M (%)	26	17.4	11	5 13 14.7
$f(g)_{MAX}$	—	—	2.4	10 2.4 1.7

Finally, from the study of nano-crystalline Li-Zn and cobalt ferrite films, we conclude that in spinel ferrite thin film magnetization is strongly dependent on texture and microstructure. The discrepancy between bulk and film magnetizationin spinel ferrite thin films is well correlated to texture (grain boundary character distribution) and microstructure (grain-size dependent volume fraction of crystallites and inter-crystalline components). In the absence of orientation effect, as in non-textured films, magnetization is shown to be grain-size dependent. In presence of varying degree of texturing in similar grain-sized films, $_M$ is correlated to grain boundary character distribution. In cases where increased film magnetization is associated with grain growth and increased texturing, $_M$ reduction is ascribed to grain-size and GBCD.The origin of lower magnetization in nano-crystalline inverse spinel ferrite films, in comparison to corresponding bulk values, have been explained here quite satisfactorily in terms of texture and microstructure of the films for the first time.

Acknowledgements

This work has been carried out as a part of Ph.D. thesis. Author would like to thank Director, RRCAT, for giving permission for carrying out of this work. The Author is grateful to his thesis supervisors Prof. N. Venkataramani and Prof.I. Samajdar, IIT Bombay and Dr. S. B. Roy and Shri R. S. Shinde, RRCAT, Indore for valuable guidance, critical analysis and support for this work.

References

1. Goldman, A. (Ed.), Modern Ferrite Technology, 2nd edition, Van NostrandReinbold, USA, (1990).
2. T. Watanabe,'Grain boundary design and grain boundary character distribution in textured polycrystalline materials', Textures and Microstructures, 14-18, 739 (1991).
3. J. Dash, Shiva Prasad, N. Venkataramani, R. Krishnan, PranKishan, Nitendar Kumar, S. D. Kulkarni and S. K. Date,'Study of magnetization and crystallization in sputter deposited LiZn ferrite thin films', J. Appl. Phys. 86, 3303 (1999).
4. Mark R. De Guire, Robert C. O'Handley, and Gretchen Kalonji, 'Cooling rate dependence of cation distributions in $CoFe_2O_4$', J. Appl. Phys. **65**, 3167 (1989).
5. H. J. Bunge (Ed.), 'Texture analysis in materials science: mathematical methods', Butterworths Publication, London (1982).
6. S. Chikazumi, and S. H. Charap, Physics of Magnetism, Wiley, New York, p. 274 (1964).
7. L.Aditya, J. Nanda, I. Samajdar, N. Venkataramani, and Shiva Prasad, 'Correlation of grain boundary nature with magnetization in RF-sputtered lithium-zinc ferrite thin films',J. Magn.andMagn.Mater., 321, 3373 (2009).
8. K. Pawlik,'Determination of the orientation distribution function from pole figures in arbitrarily defined cells', Phys. Status Solidi B 134, 477(1986).
9. L. Aditya, A. K. Srivastava, S. Sahoo, C. Mukherjee, V. R. Reddy, R. S. Shinde, A. Gupta, Shiva Prasad, I. Samajdar, R. V. Nandedkar, and N. Venkataramani, 'Growth of textured nano-crystalline cobalt ferrite thin films by pulsed laser deposition', J. Nanosci. Nanotechnol. 8, 4135 (2008).
10. P. Parayanthal, F. H. Pollak,'Raman Scattering in Alloy Semiconductors: "Spatial Correlation" Model', Phys. Rev. Lett. **52,** 1822 (1984).